Nanoscale Res Lett (2007) 2:609–613
DOI 10.1007/s11671-007-9103-3

NANO EXPRESS

Influence of GaAs Substrate Orientation on InAs Quantum Dots: Surface Morphology, Critical Thickness, and Optical Properties

B. L. Liang · Zh. M. Wang · K. A. Sablon · Yu. I. Mazur · G. J. Salamo

Received: 12 September 2007 / Accepted: 22 October 2007 / Published online: 6 November 2007
© to the authors 2007

Abstract InAs/GaAs heterostructures have been simultaneously grown by molecular beam epitaxy on GaAs (100), GaAs (100) with a 2° misorientation angle towards [01−1], and GaAs (n11)B (n = 9, 7, 5) substrates. While the substrate misorientation angle increased from 0° to 15.8°, a clear evolution from quantum dots to quantum well was evident by the surface morphology, the photoluminescence, and the time-resolved photoluminescence, respectively. This evolution revealed an increased critical thickness and a delayed formation of InAs quantum dots as the surface orientation departed from GaAs (100), which was explained by the thermal-equilibrium model due to the less efficient of strain relaxation on misoriented substrate surfaces.

Keywords Molecular beam epitaxy · InAs quantum dots · Photoluminescence · Vicinal surface

Introduction

Self-assembled InGaAs/GaAs semiconductor quantum dots (QDs) attracted extensive research efforts due to their unique properties as "artificial atoms" [1–3]. Understanding and controlling the growth of InGaAs/GaAs QDs were important both for fundamental studies and in view of their potential in optoelectronic device applications. In this arena, it is well known that the GaAs substrate orientation has a large impact on the formation and properties of the self-assembled InGaAs QDs [4–8]. This is due to the different oriented substrate surfaces that are characterized by different chemical potentials thus affecting the kinetics of adsorption, migration, desorption, reconstruction, and strain relaxation [9–12]. These differences, in turn, introduce new optical properties and potential applications [13–16].

To date, there are many experimental and theoretical studies on the influence of GaAs substrate orientation on the QDs. However, the formation and evolution of QDs on misoriented substrates remain an interesting topic because they provide insight for designing a QD device system [17]. Previously, Henini's group developed the thermal-equilibrium model [18] and theoretically proved that the critical thickness of forming InAs QDs on high index surfaces increased as the substrate orientation departed from the GaAs (100) [19]. This proof was reinforced experimentally on GaAs (511)B surface (substrate misorientation of 15.8°) and GaAs (311)B surface (substrate misorientation of 25.2°) [19, 20]. Nonetheless, our recent investigation of InAs QDs grown on patterned substrate showed that, with the misorientation angle less than 15°, the InAs QDs prefer to nucleate on the vicinal surface rather than on GaAs (100) [21, 22]. In this case, it seems that the critical thickness of forming InAs QDs on the vicinal surface is less than that on planar GaAs (100). Thereafter, one question appeared: does the thermal-equilibrium model still work well for the substrates with misorientation angle smaller than 15.8°? To verify this, InAs have been simultaneously deposited on GaAs (100), GaAs (100) with a 2° misorientation angle towards [01−1] direction and GaAs (n11)B (n = 9, 7, 5) substrates. From the atomic force microscope (AFM) characterization and photoluminescence (PL) investigation, a clear evolution from QDs to quantum well (QW) was observed while the

B. L. Liang (✉) · Zh. M. Wang · K. A. Sablon · Yu. I. Mazur · G. J. Salamo
Physics Department, University of Arkansas, Fayetteville, AR 72701, USA
e-mail: bliang@unm.edu

substrate misorientation angle increased from 0° to 15.8°. This evolution proved that the critical thickness increased as the substrate orientation departed from the GaAs (100).

Experiments

The samples used in this investigation were grown by solid-source molecular beam epitaxy (MBE) on GaAs (100), GaAs (100) with a 2° misorientation towards [01−1] and GaAs (n11)B (n = 9, 7, 5) substrates. As shown in Table 1, the substrate misorientation angle θ, increased from 0° to 2°, 8.9°, 11.4°, and 15.8°, respectively. For convenience, they were labeled samples A, B, C, D, and E. The growth was carried out simultaneously on five substrates soldered on the same molybdenum block side by side to guarantee identical growth conditions. After loading the molybdenum block into the MBE growth chamber, the surface oxide was thermally desorbed at 600 °C. Thereafter, a 0.5-μm-thick GaAs buffer layer was grown at 600 °C followed by a reduction of the substrate temperature to 530 °C for the growth of 1.6 monolayer (ML) of InAs. By in situ reflection high-energy electron diffraction, the growth rate of InAs was deduced to be 0.013 ML/s and the QD formation was confirmed on GaAs (100) surface. After 15 s of growth interruption, a 20 nm GaAs capping layer was grown on top of the QDs layer before the substrate temperature was raised to 600 °C for the growth of an additional 80 nm of GaAs capping layer. Finally, an identical InAs QD layer was again deposited at 530 °C on top of the GaAs for morphology characterization by AFM. The PL measurements were performed in a variable temperature (10–300 K) closed-cycle cryostat under the excitation of a continuous-wave YAG laser with an operated-wavelength of 532 nm. The PL spectra were analyzed by a 0.5-m spectrometer and were detected by a liquid nitrogen cooled CCD camera.

Results and Discussion

Illustrated in Fig. 1 are the AFM images and the histograms of QD height. Clearly, the surface morphology strongly depended on the substrate orientation. As shown by Fig. 1a and b, for sample A grown on planar GaAs (100), two families of InAs QDs formed on the GaAs (100)

Table 1 Substrates and misorientation angles for samples A–E

Sample #	A	B	C	D	E
Substrate	(100)	2°-[011]	(911)B	(711)B	(511)B
θ (°)	0	2	8.9	11.4	15.8

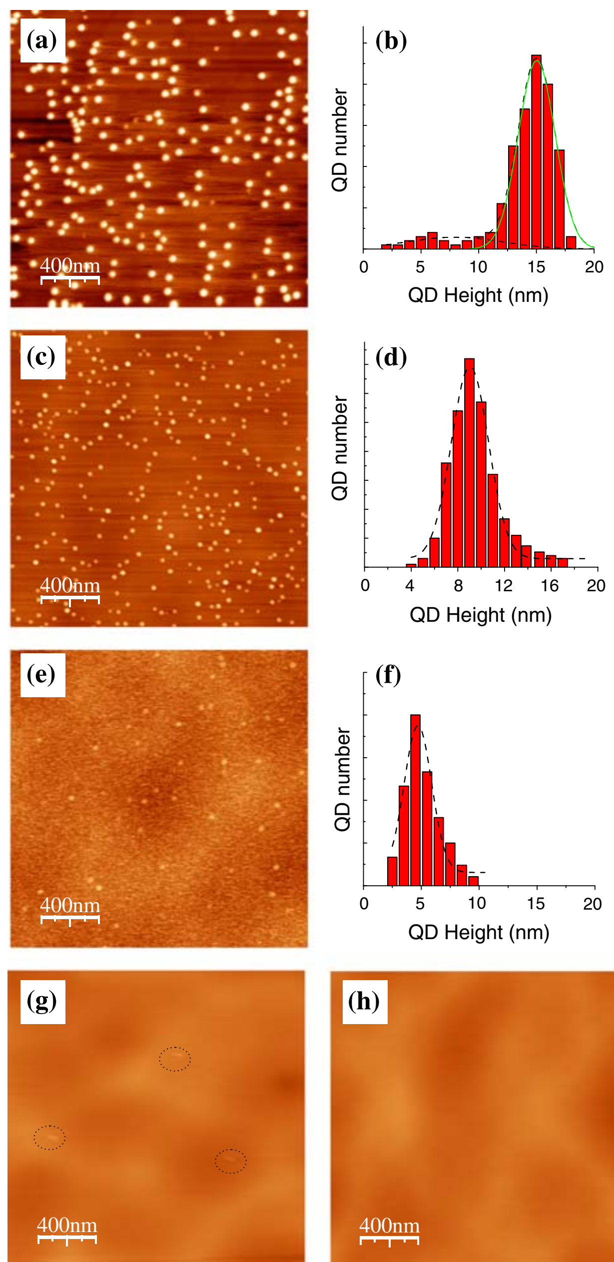

Fig. 1 (**a**) AFM and (**b**) histogram of the QD height of sample A; (**c**) AFM and (**d**) histogram of the QD height of sample B; (**e**) AFM and (**f**) histogram of the QD height of sample C; (**g**) AFM of sample D; (**h**) AFM of sample E

surface. The bigger QDs had a density of 5.2 × 10^9 cm^{-2}, a lateral size of (80.0 ± 8.6) nm and an average height of (14.7 ± 1.0) nm. The smaller QDs had a density of 4.0 × 10^8 cm^{-2}, a lateral size of (57.2 ± 10.8) nm and an average height of (6.1 ± 2.5) nm. The formation of two families of QDs was attributed to two growth mode transition onsets at 1.45 and 1.59 ML of InAs coverage [23]. For sample B, as shown by Fig. 1c and d InAs QDs were also observed on the surface, but the QDs exhibited a single-modal distribution with a density of 5.8 × 10^9 cm^{-2},

a lateral size of (51.1 ± 6.4) nm and an average height of (8.8 ± 1.4) nm. When the substrate misorientation angle increased to 8.9°, i.e., for the sample C grown on GaAs (911)B, as shown in Fig. 1e and f, the obtained QDs still exhibited single-modal distribution, but with a low density of 1.0×10^9 cm^{-2} and a small average height of (5.2 ± 1.7) nm. Clearly, the QDs on (911)B surface were closer to the two-three dimensional (2D−3D) growth mode transition than the QDs did on samples A and B. When the substrate misorientation angle further increased to 11.4° and 15.8°, i.e., for samples D and E, as shown by the AFM images in Fig. 1g and h there were no QDs found. The InAs growth was still 2D growth and QW was formed on each surface. In summary of the AFM images in Fig. 1, a continuous morphology evolution from QDs to QW was clearly observed while the substrate misorientation angle increased from 0° to 15.8°.

Then low temperature ($T = 10$ K) PL spectra was measured to verify the substrate orientation dependence and the results are given in Fig. 2a. Each PL spectrum, which was excited with a laser intensity of 0.3 W/cm^2, was normalized to its maximum. For sample A, the broad PL band around 1.1 eV was related to InAs QDs, which exhibited a bimodal distribution and agreed with the AFM observation. The peak at 1.058 eV with a FWHM of 30 meV and the peak at 1.117 eV with a FWHM of 59 meV were attributed to the big QDs and the small QDs, respectively. The narrow peak at 1.436 eV originated from the wetting layer (WL). For sample B, the PL signal showed one QD peak centered at 1.201 eV with a FWHM of 49 meV and one WL peak centered at 1.432 eV with a FWHM of 12.6 meV. For sample C, similarly, the PL spectrum showed one QD peak at 1.291 eV with a FWHM of 93 meV and a WL peak at 1.431 eV with a FWHM of 12.8 meV. However, its QD peak had a big blue-shift and less intensity. It can be seen that, from sample A to C, as the density and size of QDs decreases, their PL emission became less intense and blue-shifted. When the misorientation angle further increased to 11.4° and 15.8°, as shown in Fig. 2 there was no QD PL peak observed. Only the QW PL was founded for samples C and D. Therefore, the PL spectra in Fig. 2a also showed a clear evolution from QDs to QW while the substrate changed from GaAs (100) to GaAs (511)B, which was coincident with the AFM observation in Fig. 1.

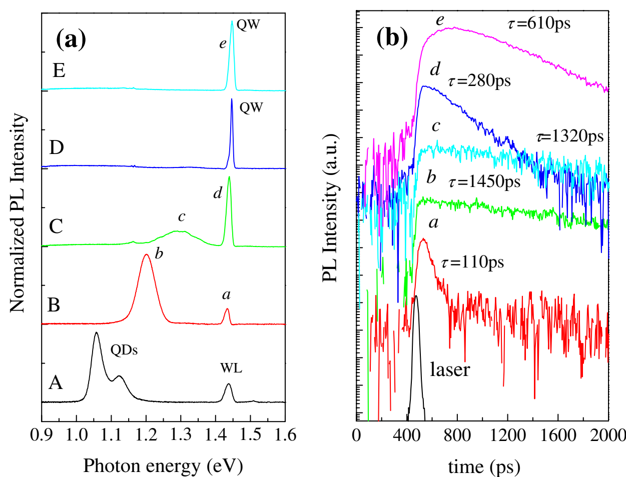

Fig. 2 (**a**) Low temperature ($T = 10$ K) PL spectra obtained with laser excitation power of 0.3 W/cm^2; (**b**) TRPL for samples B, C, and E

To further examine the optical properties, samples B, C and E were selected to measure the temporal PL (TRPL) behaviors. The measured PL band positions were indicated by the letters in Fig. 2a and the corresponding TRPL data were plotted in Fig. 2b. For sample B, its WL emission, as shown by the curve-*a*, had a decay time as short as 110 ps. This short decay time was due to the fast exciton relaxation from the WL to the confined energy states of QDs. The QD PL band at 1.201 eV had a decay time of 1,450 ps as shown by the curve-*b*, which is a typical value for InAs QDs. For sample C, its QD peak at 1.291 eV was characterized by a QD decay time of 1,320 ps as shown by curve-*c*. However, as shown by the curve-*d* its WL PL has a decay time of 280 ps, which is longer than the WL decay time obtained from curve-*a*. This long WL decay time is likely due to the very low QD density on (911)B surface. Consequently, only a small fraction of the photon-generated electron–hole pairs can recombine through the islands, and most of them have to recombine through the WL [24]. Finally, for sample E, there are no QDs. The PL band at 1.446 eV was characterized by a decay time of 640 ps, which means a typical QW characterization. The evolution from QDs to QW was further proved by the TRPL measurement while the substrate orientation changed from GaAs (100) to GaAs (511)B. Interestingly, in this investigation not only typical QW and QDs but also certain intermediate state between QW and QDs was observed. The sample grown on (911)B surface could be regarded as an example, which has a low density of small QDs with weak PL emission and a strong WL signal with a life time between the typical QW and WL of InAs QDs.

Finally, the evolution of InAs QDs formation was evident by the temperature dependence of the PL measurements. Fig. 3 strengthened the physical picture with the integrated PL intensity as a function of temperature. For sample B, the integrated intensity of its QD PL band started to quench quickly after the temperature is higher than 160 K. This is a feature for InAs QDs due to the strong 3D confinement, which demonstrates the ~12 meV exciton binding energy in these dots. Due to the fact that the excitons in the WL easily interacted with the phonon and quenched, the integrated PL intensity of the

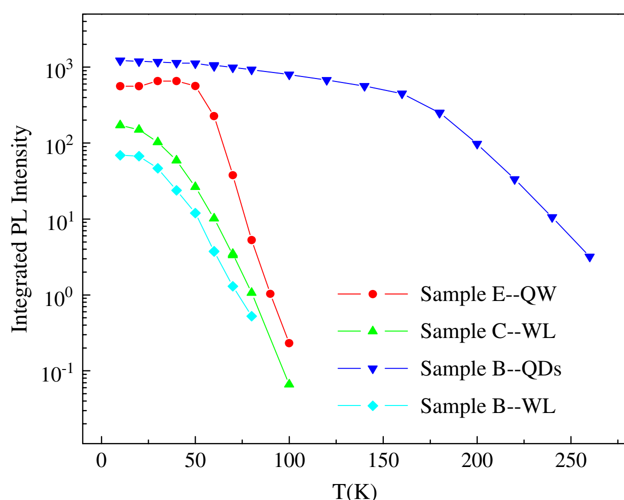

Fig. 3 Temperature dependence of integrated PL intensity

WL of sample B began to rapidly decrease as the temperature increased from 10 K. For the sample E with only QW grown on (511)B, the PL started to fast quench from the temperature of 60 K due to the relatively lower binding energy of the excitons in QW. More interestingly, we observed the temperature dependence behavior of the WL of sample C is between the typical QW of sample E and the typical WL of InAs QDs on sample B, which confirms that the sample grown on (911)B can be regarded as an intermediate state.

In summary, a clear evolution from QDs to QW was observed while the substrate varied from GaAs (100) to GaAs (511)B. To our knowledge, it is the first time that such a detailed evolution was observed by AFM, PL, and TRPL together. Since the growth condition and the InAs deposition were identical for all of the samples, we attributed this evolution due to the variation of the critical thickness on misoriented substrates. As the substrate misorientation angle increased from 0° to 15.8°, our results indicated a delayed formation of InAs QDs, which means an increased critical thickness. This observation agrees with Sanguinetti's reports, in which the critical thickness increased as the substrate varied from GaAs (511)B to GaAs (311)B [20].

Generally, the formation of self-assembled InAs QDs is explained in terms of a thermal-equilibrium picture where the system assumes the state of lowest free energy. The net energy of a QD has been defined as [18, 25]:

$$E_{QD} = E_{elastic} + E_{surface} + E_{edge},$$

where $E_{elastic}$ is the elastic energy relief due to partial strain relaxation inside the QD, $E_{surface}$ is the surface energy associated with increased surface area of the QD, and E_{edge} is the energy associated with the various facets and the resulting edges of the QD. During the SK growth of InAs QDs, the main driving force forming islands is the strain relaxation, which permits relief of part of the strain induced by the lattice mismatch between the epitaxial InAs layer and the GaAs substrate. As mentioned earlier, different oriented substrate surfaces are characterized by different chemical potentials thus affecting the kinetics of adsorption, migration, desorption, reconstruction, and strain relaxation. In fact, the in-QD strain relaxation is influenced by the substrate orientation and it has been proven that the strain relaxation is less efficient for islands grown on high index surfaces [20]. For further evidence, the aspect ratio Q (height over width) for the samples was examined. The QDs grown on substrate with larger misorientation angle appeared flatter and exhibited a lower aspect ratio ($Q \sim 0.09$ on GaAs (911)B and $Q \sim 0.17$ on GaAs (811)B) with the GaAs (100) case ($Q \sim 0.18$ for big QDs and $Q \sim 0.11$ for small QDs), which illustrate less strain relaxation for high index surfaces [19]. The inhibition of strain relaxation inside the islands, by increasing the island internal energy term, should determine a delay in the 3D growth mode onset. As experimentally observed, the critical thickness increased as the substrate orientation departed from the GaAs (100). It can be seen that our experimental results can be well explained by the thermal-equilibrium model. The thermal-equilibrium model developed by Henini's group, not only work for the high indexed substrate with misorientation angle from 15.8° to 25.2°, but also work well for small misorientation of less than 15.8°. Therefore, such a simple model in fact accounts for many experimental reports of strain-driven island evolution on high indexed and/or vicinal substrates.

We also mentioned in the introduction that, our recent work of InAs QDs grown on patterned substrates showed that the InAs QDs prefer to nucleate on the vicinal surface as compared to the GaAs (100) surface [21, 22]. In this case, it seems that the critical thickness of forming InAs QDs on the vicinal surface is less than that on GaAs (100). However, the observations in this report prove that critical thickness increased as the substrate orientation transitioned from the GaAs (100). The developed thermal-equilibrium model by Henini's group works fine for the substrates with big or small misorientation angles. Therefore, we suppose that in our previous investigation, the fact that the InAs QDs prefer to nucleate on the vicinal surface is not due to the change of critical thickness, but due to the increasing of effective deposition of InAs. Actually, many monolayer steps characterize the vicinal surfaces. These ML steps blocked and trapped the In adatoms that migrated from the nearby planar GaAs (100) surface, which caused an increase in the InAs local coverage and make the real InAs deposition in the vicinal surface area reached the critical thickness before the planar GaAs (100) plane. Therefore, the mechanism of QD formation on the patterned substrate

with vicinal surface is different for that QD formation on the pure vicinal surfaces.

Conclusions

In conclusion, InAs quantum structures simultaneously grown on GaAs (100), GaAs (100) with a 2° misorientation angle towards [01−1], and GaAs (n11)B ($n = 9$, 7, 5) substrates have been investigated by AFM characterization and PL measurements. While the substrate misorientation angle increases from 0° to 15.8°, an evolution from QDs to QW was clearly observed in both morphologic and optical investigations. Interestingly, the sample grown on (911)B surface was observed as an intermediate state between typical QW and QD structure, which has a low density of small QDs with weak PL emission and a strong WL signal with a life time between the typical QW and normal WL of InAs QDs. These observations show that the formation and the optical properties of the quantum structures strongly depend on the substrate orientation. The InAs QDs formation was delayed while the surface orientation departs from GaAs (100), as they were reported previously on GaAs (311)B and GaAs (511)B. The evolution from the QDs to QW was attributed to the less efficient of strain relaxation on misoriented substrate surfaces. This report demonstrates, the thermal-equilibrium model developed by Henini's group, not only work for the high indexed substrate with misorientation angles from 15.8° to 25.2°, but also work well for small misorientation of less than 15.8°. Therefore, such a simple model in fact accounts for many experimental reports of strain-driven island evolution on high indexed and/or vicinal substrates.

Acknowledgment The authors acknowledge the financial support of the NSF of US (through Grant No. DMR-0520550).

References

1. D. Leonard, M. Krishnamurthy, C.M. Reaves, S.P. Denbaars, P.M. Petroff, Appl. Phys. Lett. **63**, 3203 (1993)
2. Z. Yuan, B.E. Kardynal, R.M. Stevenson, A.J. Shields, C.J. Lobo, K. Cooper, N.S. Beattie, D.A. Ritchie, M. Pepper, Science **295**, 102 (2000)
3. S.S. Li, J.B. Xia, Z.L. Yuan, Z.Y. Xu, W.K. Ge, Y. Wang, J. Wang, L.L. Chang, Phys. Rev. B. **54**, 11575 (1996)
4. M. Henini, Nanoscale Res. Lett. **1**, 32 (2006)
5. Y. Okada, M. Miyagi, K. Akahane, Y. Luchi, J. Appl. Phys. **90**, 192 (2001)
6. Y. Temko, T. Suzuki, P. Kratzer, K. Jacobi, Phys. Rev. B **68**, 165310 (2003)
7. S.P. Guo, H. Ohno, A. Shen, F. Matsukura, Y. Ohno, Appl. Phys. Lett. **70**, 2738 (1997)
8. T. Kitada, Y. Tatsuoka, S. Shimomura, S. Hiyamizu, J. Vac. Sci. Technol. B **18**, 1579 (2000)
9. D.I. Lubyshev, P.P. González-Borrero, E. Marega Jr., E. Petitprez, P. Basmaji, J. Vac. Sci. Technol. B **14**, 2212 (1996)
10. M. Henini, S. Sanguinetti, S.C. Fortina, E. Grilli, M. Guzzi, G. Panzarini, L.C. Andreani, M.D. Upward, P. Moriarty, P.H. Beton, L. Eaves, Phys. Rev. B. **57**, R6815 (1998)
11. W. Jiang, H. Xu, B. Xu, W. Zhou, Q. Ghou, D. Ding, J. Liang, Z.G. Wang, J. Vac. Sci. Technol. B **19**, 197 (1996)
12. S.S. Li, J.B. Xia, Phys. Rev. B **50**, 8602 (1994)
13. Zh.M. Wang, Sh. Seydmohamadi, J.H. Lee, G.J. Salamo, Appl. Phys. Lett. **85**, 5031 (2004)
14. J.S. Lee, M. Sugisaki, H.W. Ren, S. Sugou, Y. Masumoto, Physica E **7**, 303 (2000)
15. M. Kawabe, K. Akahane, S. Lan, K. Okino, Y. Okada, H. Koyama, Jpn. J. Appl. Phys. **38**, 491 (1995)
16. S. Martini, A.A. Quivy, A. Tabata, J.R. Leite, J. Appl. Phys. **90**, 2280 (1998)
17. B.D. Min, Y.K.E.K. Kim, S.K. Min, M.J. Park, Phys. Rev. B. **57**, 11879 (1998)
18. I. Daruka, A.L. Barabasi, Phys. Rev. Lett. **79**, 3708, 1997
19. S. Sanguinetti, G. Chiantoni, E. Grilli, M. Guzzi, M. Henini, A. Polimeni, A. Patane, L. Eaves, P.C. Main, Europhys. Lett. **47**, 701 (1999)
20. S. Sanguinetti, G. Chiantoni, E. Grilli, M. Guzzi, M. Henini, A. Polimeni, A. Patane, L. Eaves, P.C. Main, Mater. Sci. Eng. B **74**, 239 (2000)
21. Zh.M. Wang, J.H. Lee, B.L. Liang, W.T. Black, Vas P. Kunets, Yu I. Mazur, G.J. Salamo, Appl. Phys. Lett. **88**, 233102 (2006)
22. J.H. Lee, Zh.M. Wang, B.L. Liang, W.T. Black, Vas P. Kunets, Yu I. Mazur, G.J. Salamo, Nanotechnology **17**, 2275 (2006)
23. F. Arciprete, E. Placidi, V. Sessi, M. Fanfani, F. Patella, A. Balzarotti, Appl. Phys. Lett. **89**, 041904 (2006)
24. M.J. da Silva, A.A. Quivy, P.P. Gonzalez-Borrero, N.T. Moshegov, E. Marega Jr., J. Cryst. Growth **227–228**, 1025 (2001)
25. N. Moll, M. Scheffler, E. Pehlke, Phys. Rev. B. **58**, 4566 (1998)